

Variability of effects of spatial climate data aggregation on regional yield simulation by crop models

H. Hoffmann^{1,*}, G. Zhao¹; L. G. J. van Bussel^{1,2}, A. Enders¹, X. Specka³, C. Sosa⁴, J. Yeluripati^{5, 16}, F. Tao⁶, J. Constantin⁷, H. Raynal⁷, E. Teixeira⁸, B. Grosz⁹, L. Doro¹⁰, Z. Zhao¹¹, E. Wang¹¹, C. Nendel³, K. C. Kersebaum³, E. Haas¹², R. Kiese¹², S. Klatt¹², H. Eckersten¹³, E. Vanuytrecht¹⁴, M. Kuhnert⁵, E. Lewan⁴, R. Rötter⁶, P. P. Roggero¹⁰, D. Wallach⁷, D. Cammarano¹⁵, S. Asseng¹⁵, G. Krauss¹, S. Siebert¹, T. Gaiser¹, F. Ewert¹

¹Crop Science Group, Institute of Crop Science and Resource Conservation (INRES), University of Bonn, Katzenburgweg 5, 53115 Bonn, Germany

²⁻¹⁶Co-author addresses are provided in the Supplement (www.int-res.com/articles/suppl/c065p053_supp.pdf)

ABSTRACT: Field-scale crop models are often applied at spatial resolutions coarser than that of the arable field. However, little is known about the response of the models to spatially aggregated climate input data and why these responses can differ across models. Depending on the model, regional yield estimates from large-scale simulations may be biased, compared to simulations with high-resolution input data. We evaluated this so-called aggregation effect for 13 crop models for the region of North Rhine-Westphalia in Germany. The models were supplied with climate data of 1 km resolution and spatial aggregates of up to 100 km resolution raster. The models were used with 2 crops (winter wheat and silage maize) and 3 production situations (potential, water-limited and nitrogen-water-limited growth) to improve the understanding of errors in model simulations related to data aggregation and possible interactions with the model structure. The most important climate variables identified in determining the model-specific input data aggregation on simulated yields were mainly related to changes in radiation (wheat) and temperature (maize). Additionally, aggregation effects were systematic, regardless of the extent of the effect. Climate input data aggregation changed the mean simulated regional yield by up to 0.2 t ha⁻¹, whereas simulated yields from single years and models differed considerably, depending on the data aggregation. This implies that large-scale crop yield simulations are robust against climate data aggregation. However, large-scale simulations can be systematically biased when being evaluated at higher temporal or spatial resolution depending on the model and its parameterization.

KEY WORDS: Spatial aggregation effects · Crop simulation model · Input data · Scaling · Variability · Yield simulation · Model comparison

Resale or republication not permitted without written consent of the publisher

1. INTRODUCTION

Process-based crop models have typically been developed for the field scale, for which model-driving variables (e.g. soil variables) are easily obtained (Van Ittersum et al. 2003, Hansen et al. 2006). However,

crop models are increasingly used for large-scale simulations (Chipanshi et al. 1999, Folberth et al. 2012). In the following, scale refers to the spatial extent and resolution of a given grid cell size, ignoring temporal scales (van Bussel et al. 2011a, Weiermüller et al. 2011). Thus, using field-scale crop mod-

els with input data at scales other than what they were developed for raises the question of how the choice of scale influences the simulation outputs. Changing the spatial resolution by aggregation or disaggregation of data bears the risk of missing the relevant scale of particular processes or phenomena that are often scale dependent (Meentemeyer 1989).

Although the relevance of scale (Hansen & Jones 2000, Ewert et al. 2011, Nendel et al. 2013) and spatial data aggregation (Gardner et al. 1982, Cale et al. 1983, Cale & O'Neill 1988, Rastetter et al. 1992, Pierce & Running 1995, Nungesser et al. 1999, Gong et al. 2003, Syphard & Franklin 2004, Lorite et al. 2005, Ershadi et al. 2013) is well known and data aggregation has been addressed, for instance, in soil or hydrological process modelling (Heuvelink & Pebesma 1999, Haverkamp et al. 2005, Leopold et al. 2006, Bormann et al. 2009), few studies have characterized the effect in application of crop models with spatially aggregated climate input data on simulated regional yields, hereafter called the aggregation effect. For example, De Wit et al. (2005) used precipitation and radiation aggregated from 10 to 50 km resolution as model input to simulate winter wheat and grain maize yields in Germany and France. These yields showed a root mean square error (RMSE) of 0.33 t ha⁻¹ ($R^2 > 0.96$) and a low bias between results from 10 and 50 km resolutions (estimated from Fig. 4 in De Wit et al. 2005). This low bias is in agreement with Folberth et al. (2012), who found small differences in maize yields in the USA within resolutions of 7.5 to 45 km. Angulo et al. (2013) also found small differences in spring barley yields in Finland within resolutions of 10 to 100 km. Similarly, Van Bussel et al. (2011b) reported a low bias in simulated wheat phenology using aggregated temperatures and sowing dates. Eyshi Rezaei et al. (2015) concluded that heat and drought stress effects on wheat yield are sufficiently determined at 100 km resolution. Thus, aggregation of climate input data at resolutions of 10 to 100 km can be expected to have a low impact on crop model output, for instance in large-scale simulations. This threshold holds true for the situations and models investigated, but has not been generalized. Since data aggregation may destroy physical consistency (Hoffmann & Rath 2012) or combine data beyond the meaningful range of the underlying process, the latter may be taken into account by keeping aggregated grid sizes below the range estimated via semivariogram models (Brown et al. 1993, Artan et al. 2000). While previous studies indicated the spatial resolution at which crop models may be applied without larger errors in the average simulated crop

yields, that research only represented a small sample of crop models and output variables. Most studies used 1 specific crop model. Furthermore, the systematic behaviour of aggregation effects of models across scales, production situations or crops has not been quantified beyond reporting magnitude and distribution.

We hypothesized that crop models differ in their sensitivity to climate input data aggregation, as well as in the fraction of explained variance of the aggregation effects. However, it is unknown whether this affects regional yield estimates from simulations in a systematic way. The objective of this work was therefore to compare the response of regional yields simulated by crop models to climate input data aggregation and to propose a measure for the systematic proportion of the aggregation effects.

2. METHODS

2.1. Procedure and regional focus

The hypotheses given above were tested in the state of North Rhine-Westphalia (NRW, Fig. 1), one of the larger federal states of Germany with a total area of 34 098 km² (Cologne District Council 2013). NRW is characterized by a humid, temperate climate and heterogeneous topography with elevations between 9 and 843 m a.s.l., resulting in several agro-ecological zones with different temperature and rainfall regimes. In order to assess spatial aggregation effects, climate input data were aggregated to spatial resolutions varying between 1 and 100 km (Fig. 2) and used for driving crop models for simulations of winter wheat *Triticum aestivum* L. and silage maize *Zea mays* L. for the entire state (Fig. 2). Aggregation effects were estimated by relating model output variables to varying climate inputs. Finally, main determinants of these aggregation effects were identified by analysing the relative contributions of the climate variables and separately analysing the relative importance of model variables employing partial least squares (PLS) regression.

2.2. Climate data processing, aggregation and characterization

Time series of daily minimum, mean and maximum air temperature (2 m above ground), precipitation, global radiation, wind speed and relative humidity for the period 1982–2011 from 280 daily weather sta-

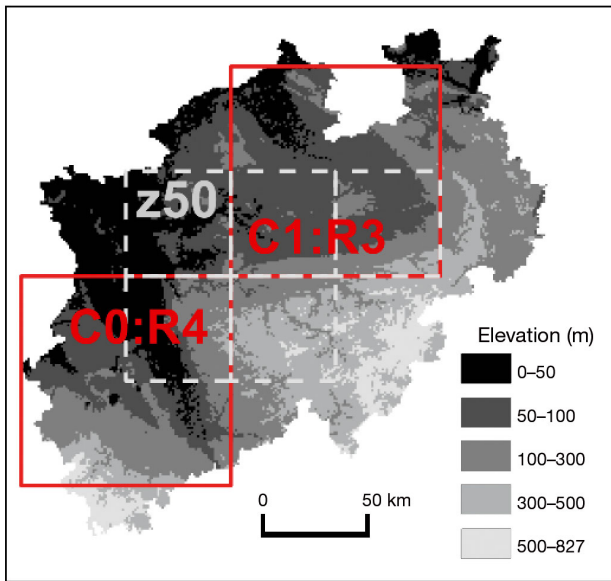


Fig. 1. North Rhine-Westphalia, Germany. Squares display selected areas used to validate results at the state level: 2 subregions (C0:R4 and C1:R3, 100 km, solid red outline) and 1 subregion (z50) consisting of 5 grid cells (50 km resolution, grey dashed outline)

tions, as well as an interpolated grid of 1 km resolution of monthly time series were obtained from the German Meteorological Service. The monthly grids were combined with the daily weather station data as

described by Zhao et al. (2015a). Regional climate properties for the different resolutions are given by Table 1.

Daily climate data in spatial resolution α of 1 km² were spatially averaged for 4 different coarser grid sizes of 10, 25, 50 and 100 km (for equations, see the Supplement at www.int-res.com/articles/suppl/065p053_supp.pdf). Coarser grids were technically set up starting in the northwest corner of the study region.

In order to detect any possible aggregation of spatially incoherent data, the climate was characterized by semivariograms, which provide information about the extent of spatial dependency (Brown et al. 1993). This so-called range was estimated by fitting Gaussian (precipitation, temperature) and exponential (global radiation) variogram models to the empirical semivariance (Wackernagel 1995, Webster & Oliver 2001, Minasny & McBratney 2005).

Due to incomplete data coverage beyond NRW, data means of grid cells of resolutions larger than 1 km and thus crossing the boundary of the state might be biased, depending on the grid cell size and data coverage (see Fig. S3 in the Supplement). Therefore, all calculations were validated with the help of sub-regions, i.e. 2 cells of 100 km resolution and a spatial data coverage of >80 % (C0:R4 and C1:R3, Fig. 1) and 5 cells of 50 km resolution with a corresponding coverage of 100 % (z50, Fig. 1).

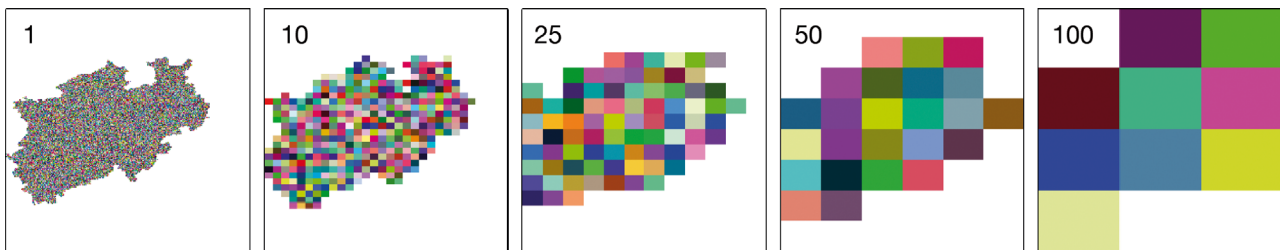


Fig. 2. Climate data resolution (1, 10, 25, 50 and 100 km) used as input for crop models

Table 1. Climate of North Rhine-Westphalia, Germany (1982–2011, not area weighted). Standard deviations (σ) are calculated from all grid cells and years of a corresponding resolution

Scale (km)	Annual precipitation (mm yr ⁻¹)		Daily temperature (°C)		Annual global radiation (MJ m ⁻² yr ⁻¹)	
	Mean	σ	Mean	σ	Mean	σ
1	898.9	214.0	9.7	1.2	3758.0	169.4
10	881.7	204.0	9.6	1.2	3757.1	166.8
25	873.1	191.9	9.5	1.2	3756.6	163.8
50	853.8	170.8	9.4	1.1	3754.0	162.0
100	824.4	149.8	9.4	1.0	3765.5	160.6

2.3. Crop simulations

In our study, 13 models currently used for addressing different research questions at various scales were selected (Table 2 and see Table S1 [link in the Supplement, Section 3]). This model ensemble was used to simulate development, growth and yield for the period 1982–2011 for each grid cell at each spatial resolution for wheat and maize. If not further specified in the following, yield of wheat refers to grain yield, whereas maize yield is aboveground biomass. Simulations were conducted and evaluated for (1) potential, (2) water-limited and (3) nitrogen-water-limited production situations; correspondingly limited by (1) temperature and radiation, (2) precipitation, temperature and radiation and (3) nitrogen, precipitation, temperature and radiation (Van Ittersum & Rabbinge 1997, Evans & Fisher 1999). Models were set up with a single soil profile (sandy loam; Table S2) which represents a typical deep cropland soil with high water holding capacity and with a common management for any of the grid cells (Table 3). Models were calibrated at 1 km resolution, using 1 typical sowing and 1 typical harvest date per crop as

well as the whole region weighted average wheat yield and aboveground biomass of maize derived from county statistics respectively from 1999 to 2011 and from 2000 to 2008 (Statistische Ämter des Bundes und der Länder 2013). The county statistics are point data and are partially based on expert knowledge and, therefore, are shown only for the purpose of putting the results into context.

2.4. Model intercomparison and Taylor diagrams

Crop model results were compared via Taylor diagrams (Taylor 2001), presenting the correlation coefficient R , centred root-mean-square difference (RMSD) and standard deviations σ of all grid cells and years as compared to the model ensemble mean (see the Supplement for equations). R and RMSD show correlation and difference, respectively, of each model to the model ensemble mean. Standard deviation is shown for each model as well as for the ensemble mean. Statistics were calculated from all grid cells of 1 km resolution and years, thus showing the model agreement in time and space.

Table 2. Crop models assessed in this study. For more detailed descriptions, see Table S1

No.	Model	References
1	APSIM-Nwheat	Asseng et al. (1998, 2004), Keating et al. (2003)
2	APSIM	Keating et al. (2003), Holzworth et al. (2014)
3	APSIM, modified	Wang et al. (2002), Keating et al. (2003), Chen et al. (2010)
4	AquaCrop4.0	Raes et al. (2009), Steduto et al. (2009), Vanuytrecht et al. (2014)
5	COUP	Conrad & Fohrer (2009), Jansson & Karlberg (2004)
6	DailyDayCent	Del Grosso et al. (2001, 2006), Parton et al. (2001), Yeluripati et al. (2009)
7	EPIC v. 0810	Williams (1995)
8	HERMES	Kersebaum (2007, 2011)
9	LandscapeDNDC	Haas et al. (2012), Kraus et al. (2015)
10	LINTUL5	Van Ittersum et al. (2003), Shibu et al. (2010)
11	MCWLA	Tao & Zhang (2009, 2013)
12	MONICA	Nendel et al. (2011)
13	STICS	Brisson et al. (1998, 2008), Bergez et al. (2013)

2.5. Probability density functions (PDFs)

PDFs were obtained by kernel density estimation with a Gaussian kernel (see Hoffmann & Rath 2013 for equations). In order to ensure comparability between the PDF of a given crop, the bandwidth was kept constant to 0.1 t ha⁻¹ (wheat) and 0.3 t ha⁻¹ (maize).

Table 3. Crop model settings and assumptions. Area-weighted average yield is derived from county statistics, moisture content: 0%. DOY: day of the year of a non-leap year; Initial Nmin: total mineral nitrogen of the soil profile (values differ with soil layer)

Domain	Unit	Winter wheat	Silage maize
Sowing date	DOY	274	110
Harvest date	DOY	213	263
Average yield	t ha ⁻¹	7.2	14.3
Max. rooting depth	m	1.5	1.5
Time of ploughing	–	Autumn	Autumn
Planting density	m ⁻²	400	10
Sowing depth	m	0.04	0.06
Initial soil moisture relative to available field capacity ^a	%	50	80
Initial Nmin	kg ha ⁻¹	56	56
Nitrogen fertilization	kg ha ⁻¹	130, 52, 26	30, 208
Date of fertilization	DOY	60, 105, 152	91, 152

^aSet for each soil layer

2.6. Analysis of aggregation effects

2.6.1. Mean regional effects

Climate data aggregation effects were evaluated in the climate data itself and in model outputs. For this purpose, regional means and spatial variances of daily climate data and of annual crop model outputs were calculated as absolute differences from coarser resolutions to the 1 km resolution (see the Supplement for equations). Model outputs were thus analysed only at the resolution of the input data (e.g. to calculate the spatial variance) as well as the mean of the entire region (e.g. to calculate regional yields).

2.6.2. Fraction of directed effects

We tested whether wheat and maize yields follow a specific ascending or descending order related to the order of the spatial resolution, for instance, whether yields at 100 km resolution were larger than yields at 50 km resolution and whether yields at 50 km resolution were larger than yields at 25 km resolution and so on. For this purpose, the fraction P of simulated yields monotonously following the order or inverse order of the spatial resolutions for each model was calculated (see the Supplement for equations).

2.6.3. PLS regression

While P gives insights into the direction and behaviour of aggregation effects, the relevance of factors (e.g. of single climate variables) to aggregation effects remains unclear. However, while the estimated effects and possible causes will be highly auto-correlated, regression algorithms may fail to establish statistical relations between independent (aggregated input dataset) and dependent (crop model output, e.g. yield) data (Luedeling & Gassner 2012). Additionally, the algorithm must handle a large number of independent variables, while avoiding over fitting. In order to evaluate aggregation effects, which are likely driven by numerous complementary as well as contrary processes of crop model and input data interaction, PLS regression (also known as projection to latent structures regression) was applied. PLS has been employed for similar purposes related to impacts of climate variation, i.e. on tree phenology (Luedeling & Gassner 2012, Guo et al. 2013). The method takes the dependent variable into account, selecting only the most relevant linear combinations

for regression. We thus introduce PLS as a method for quantifying the fraction of variance of aggregation effects explained by climate data or model outputs. PLS was used to assess the relative importance of the climate variables and a limited number of model variables to the aggregation effects.

Dependent variables were changes in mean yields (wheat) and final aboveground biomass (maize), whereas (1) the climate variables during the entire growing period, from sowing to anthesis and from anthesis to maturity, as well as (2) model outputs (wheat grain yield, maize aboveground biomass, maximum leaf area index, cumulative evapotranspiration, cumulative intercepted photosynthetic active radiation, duration of phenological phases) were used as independent variables. The importance of these variables to the aggregation effect was estimated calculating the variable importance for projection (VIP) from the PLS loadings (Wold 2001). The highest 5 predictors with a VIP > 1 were selected.

3. RESULTS

3.1. Climate input data: semivariance and aggregation effects

Spatial aggregation of climate time series removed climate extremes of the region, while area means were stable across resolutions (Fig. 3). Consistently, the corresponding spatial variance of the climate variables decreased with increasing spatial resolution. Daily mean temperature, global radiation and precipitation exhibit a spatial autocorrelation in the range and above the largest aggregation used in this study (Fig. 4, effective range of 93.9, 122.5 and 161.9 km for precipitation, daily mean temperature and global radiation, respectively; R^2 : 0.998, 0.997, 0.995, respectively). Aggregating the climate data decreases the semivariance, as shown for precipitation (Fig. 4).

3.2. Simulated crop yields

3.2.1. Crop-specific yields

The ensemble means of simulated wheat and maize yields of the region were in the range of 7.6 to 8.7 t ha⁻¹ and 15.4 to 17.6 t ha⁻¹, respectively, depending on the production conditions (Table 4, Fig. 5). On average, simulated yields were higher than the observed yields of 7.2 t ha⁻¹ and 14.3 t ha⁻¹, respectively.

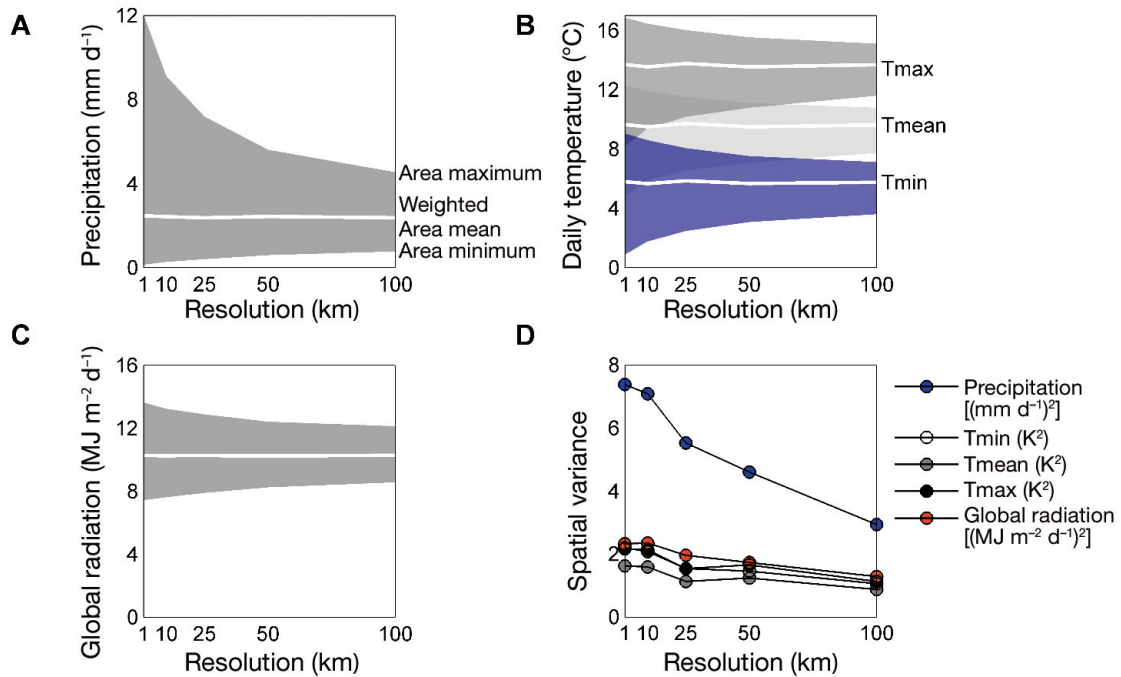


Fig. 3. Area weighted means (white lines) and ranges (minimum to maximum values, illustrated by the grey areas) of key climate variables: (A) precipitation, (B) daily temperature (Tmin, Tmean, Tmax: daily minimum, mean and maximum temperature, respectively) and (C) global radiation, as well as (D) their spatial variance as affected by data aggregation. Values are average area means and extremes

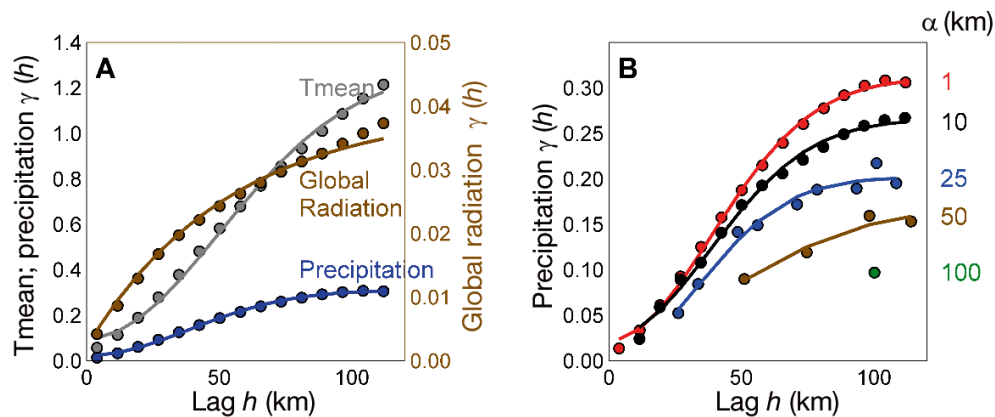


Fig. 4. Spatial dependency of selected climate variables in North Rhine-Westphalia, Germany. (A) Empirical semivariance (dots) and fitted variogram model (solid lines). A Gaussian model was fitted to daily mean temperature (Tmean) and precipitation whereas an exponential model was used for global radiation. (B) Empirical semivariance (dots) and fitted Gaussian variogram model (solid lines) for precipitation at varying resolutions α (1, 10, 25, 50 and 100 km)

3.2.2. Temporal variability

On average, crop models reproduced the year-to-year variability of simulated yields calculated from county statistics (Fig. 5). However, the majority of the models simulated a larger year-to-year variability in yields than observed. Generally, simulated temporal variations of yields were better for wheat than for maize. Single-year yield distributions are shown in Fig. S2.

3.2.3. Influence of the production situation

Yields decreased consistently from potential to water-limited to nitrogen-water-limited production (Table 4, Fig. 5). While on average, water-limited wheat and maize yields were respectively 0.4 and 1.2 t ha⁻¹ lower than potential yields, they were additionally 0.6 and 0.7 t ha⁻¹ lower under nitrogen-water-limited conditions as under water-limited conditions (Table 4). While nitrogen availability was thus

limiting yields more than water limitations, the latter were noticeably stronger in 1996, 2010 and 2011, corresponding to 74 % of the decline in these years as compared to potential conditions.

3.2.4. Spatial variability

The interquartile range of yields across the region and from all 3 production situations was in the range (maize) and partially above the range (wheat) of observations (not shown). The corresponding coefficient of variation of crop yield across the region for the mean of years was up to 8.2% and 12.9% for wheat and maize, respectively. Distributions of simulated yields across the region at 1 km resolution consistently showed a negative skew in the mean (Fig. 6).

3.2.5. Crop model variability

Simulated yields differed across models and crops, showing a higher agreement among models for wheat than for maize (Fig. 7). For wheat, most models—with the exception of DailyDayCent and LandscapeDNDC—had a standard deviation across all years and grid cells in the range of 1 t ha⁻¹, while the standard deviation of the ensemble mean was about 0.5 t ha⁻¹. Similar results were found for maize,

where models showed a larger spread in the standard deviation (approximate range 1.3 to 3.5 t ha⁻¹) compared to the ensemble mean (1.0 to 1.4 t ha⁻¹). However, models are more dispersed for potential maize aboveground biomass than for potential wheat grain yield, with only Simplace<LINTUL5> exhibiting a larger spatio-temporal standard deviation of biomass than other models. Contrastingly, while simulations for wheat varied little between production situations, simulations for maize showed an increasing standard deviation and RMSD between single models and the ensemble mean of model outputs, from potential to water-limited and nitrogen-water-limited production. However, correlation coefficients revealed a range of agreement of 0 to 0.75 and -0.5 to 0.95 for wheat and maize, respectively, underpinning the larger agreement between single models and model ensembles for wheat than for maize.

3.3. Aggregation effects

3.3.1. Crop-specific aggregation effects

Yield and biomass distributions were distinctly different for the 2 crops and were affected by aggregation (Table 4, Fig. 6). On average, aggregation of climate input data led to an increase of wheat grain yields (Fig. 8). Mean aggregation effects up to 0.2 t ha⁻¹ were found for both wheat and maize, thus resulting in a lower relative aggregation effect in relation to the yield for maize as compared to wheat (Table 4). While the mean and maximum likelihood of yield PDFs of the ensemble results over the region were hardly affected by aggregation, the width was reduced with increasing aggregation (Fig. 6). Contrary to the net aggregation effect of the region, crops differed in their PDF as aggregation led to a mode at higher yields of wheat in contrast to the PDF mode of maize.

3.3.2. Temporal variability

Single-year aggregation effects followed no clear pattern, as positive and negative aggregation effects were simulated. In some years, the aggregation effect consistently increased or decreased with the resolution (see example in Fig. S2). For instance, the annual mean yield of wheat and maize of the region followed the order of the spatial resolutions P in 50.1 % and 34.9 % of all years in the mean of models, respectively.

Table 4. Effect of climate input data aggregation on model ensemble mean and spatial variance of simulated yields

Production situation	Scale (km)	Winter wheat grain yield		Silage maize aboveground biomass	
		Mean (t ha ⁻¹)	σ^2 (t ha ⁻¹) ²	Mean (t ha ⁻¹)	σ^2 (t ha ⁻¹) ²
Potential	1	8.6	0.3	17.4	4.2
	10	8.6	0.3	17.4	3.8
	25	8.6	0.2	17.4	3.3
	50	8.6	0.2	17.5	2.5
	100	8.7	0.1	17.6	1.5
Water-limited	1	8.2	0.5	16.2	4.1
	10	8.2	0.5	16.1	3.7
	25	8.3	0.4	16.2	3.2
	50	8.3	0.3	16.3	2.4
	100	8.4	0.2	16.4	1.6
Nitrogen-water-limited	1	7.6	0.4	15.5	4.0
	10	7.6	0.4	15.4	3.6
	25	7.6	0.3	15.5	3.1
	50	7.6	0.2	15.6	2.3
	100	7.7	0.2	15.7	1.6

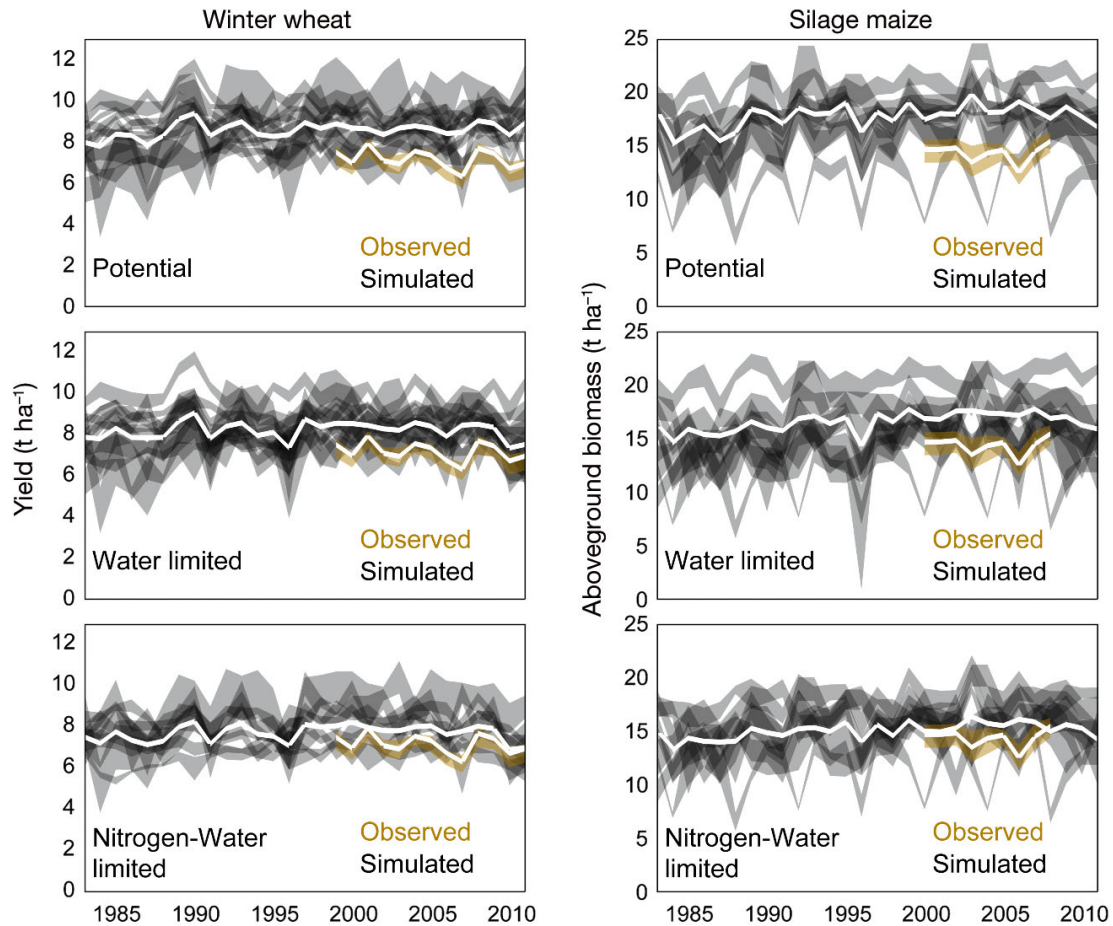


Fig. 5. Simulated wheat grain yield and maize aboveground biomass for 3 production situations (potential, water-limited and nitrogen-water-limited) at 1 km resolution, showing single model and observed 25 to 75 percentile range across the region (shaded areas), model ensemble and observed area weighted mean from county-level statistics (white lines). Areas are plotted with transparency, thus darker areas illustrate coinciding simulation results of several models or coincidence of simulation results with observations

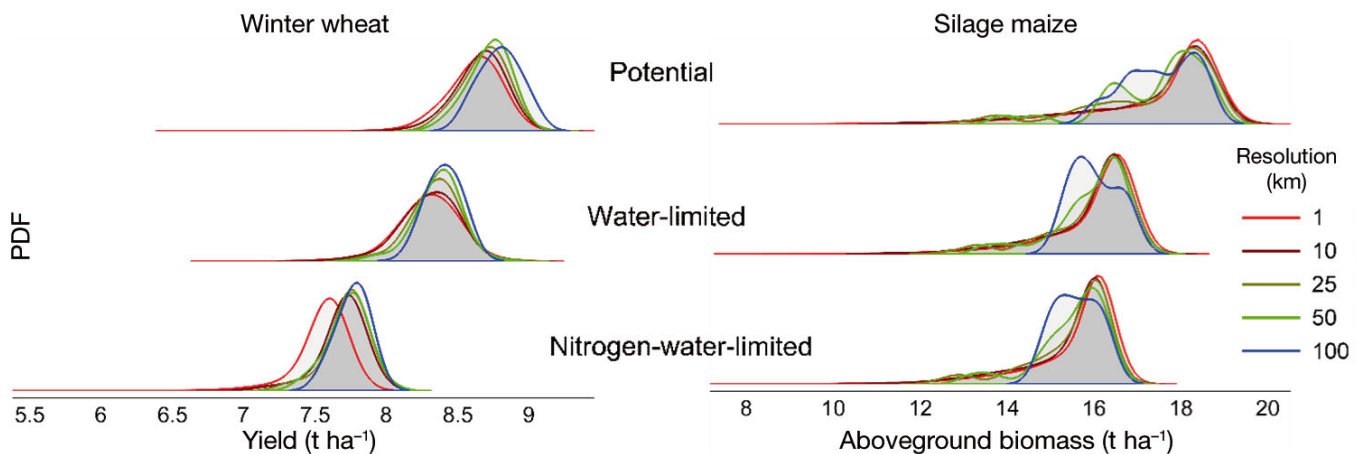


Fig. 6. Probability density functions (PDF) of simulated wheat grain yield and maize aboveground biomass. PDFs were estimated from mean grid cell yields and biomass (mean of years) using a Gaussian kernel of bandwidth 0.1 and 0.3 t ha⁻¹ for wheat and maize, respectively. Areas are plotted with transparency, thus darker areas illustrate coinciding simulations

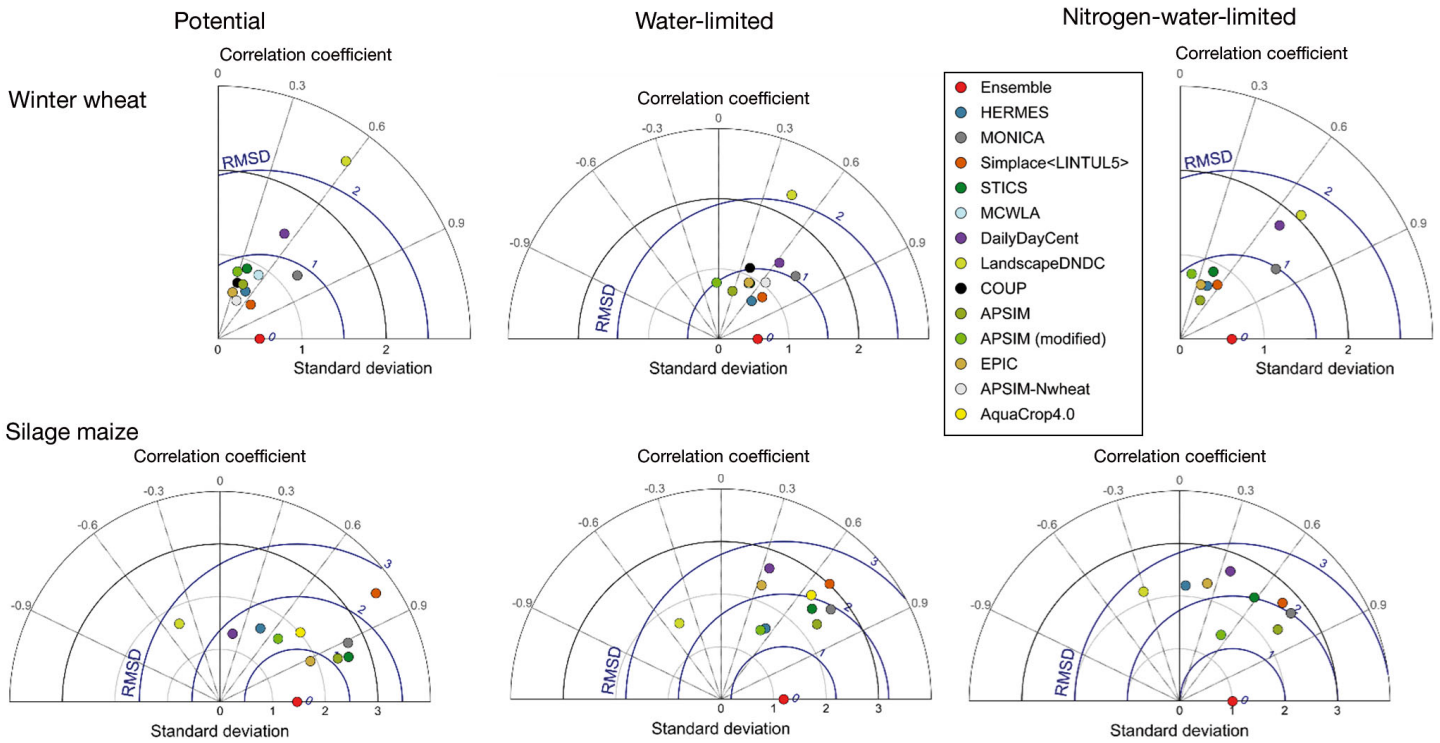


Fig. 7. Taylor diagrams of simulated wheat and maize yields from respectively 29 and 30 yr and from 34 168 grid cells (resolution $\alpha = 1$ km), showing: the standard deviation of each model (σ), the correlation between the models (R) and the centred root mean square difference (RMSD) to the ensemble mean. Denser distributions show smaller diversity among models and vice versa. RMSD and standard deviation are given in t ha^{-1} . For each model $n = 990\,872$ and $n = 1\,025\,040$ for wheat and maize, respectively

3.3.3. Spatial variability

With coarser spatial resolutions, grid cells located at the region boundary were increasingly less represented by data (Figs. 1, S1, & S3). As the number of grid cells decreases with coarser spatial resolution, a higher fraction of grid cells extends beyond the boundary of the region. However, analysing sub-regions of 50 and 100 km resolution revealed similar patterns for mean aggregation effects compared to the entire region of NRW (Fig. 8). Similar to the mean aggregation effects, extremes of aggregation effects of sub-regions were comparable to those of NRW. For maize, however, sub-region C0:R4 showed larger aggregation effects under water-limited conditions, resulting from simulations of the AquaCrop 4.0 model.

3.3.4. Influence of the production situation

Aggregation effects were similar in the median for all 3 production situations (Fig. 8), showing a similar pattern across resolutions. Again, larger aggregation effects were found under water-limited conditions for maize.

3.4. Model interaction with aggregation effects

3.4.1. Crop model interaction with crop

While aggregation effects were similar among the crops for the ensemble mean, they differed largely in their extent between models (Fig. 8, Tables 5 & 6). The range of effects was larger on average for maize than for wheat. However, some single models showed larger positive aggregation effects for maize (e.g. HERMES), comparable aggregation effects for both crops (e.g. MONICA) or lower net aggregation effects for maize (e.g. SIMPLACE<LINTUL5>).

3.4.2. Crop model interaction with time

Crop models differed substantially in their sensitivity to climate input data aggregation when single years were considered (Tables 5 & 6). Years with lowest and largest aggregation effects (Fig. S4) differed among crop models with no clear pattern. In addition, models differed in their fraction of yields following clearly the order of the resolutions, P , with models ranging from 20.0% (EPIC) to 66.1% (HERMES).

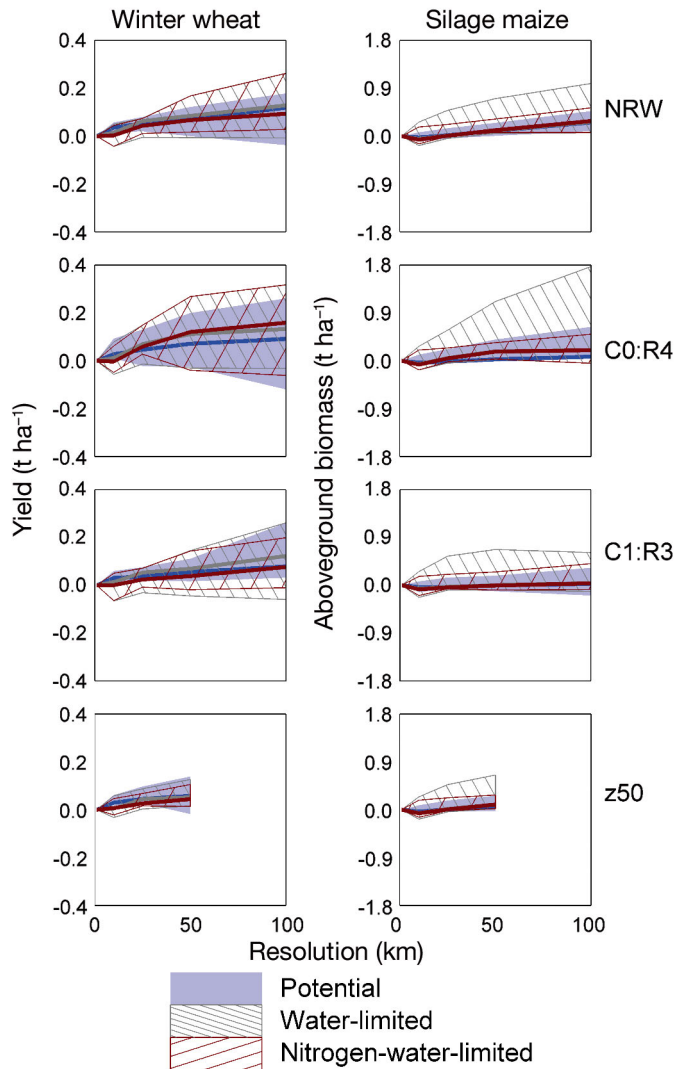


Fig. 8. Differences of wheat grain yield and maize above-ground biomass simulated with aggregated input climate data to yield and biomass simulated with climate time series at 1 km resolution of North Rhine-Westphalia, Germany, 2 subregions (C0:R4 and C1:R3, 100 km²) and 1 subregion (z50) consisting of 5 grid cells (50 km² each; see Fig. 1 for regions). The figure displays the minimum to maximum ranges over the models (shaded and hatched areas) and the ensemble median (thick lines). Values are mean values of 1983–2011

As compared to 1.7% probability for a randomly ascending or descending sequence out of 120 permutations, the results indicate systematic processes. Ranking models from high to low systematic effects for wheat yields according to *P* results in the following order: STICS > APSIM(modified) > APSIM > SIMPLACE<LINTUL5> > LandscapeDNDC > HERMES > APSIM-Nwheat > MONICA > COUP > EPIC > MCWLA > DailyDayCent. For maize aboveground

biomass the order is: HERMES > LandscapeDNDC > AquaCrop4.0 > DailyDayCent > SIMPLACE<LINTUL5> > STICS > APSIM(modified) > MONICA > EPIC > APSIM.

3.4.3. Crop model interaction with space

Differences in the interaction between models and the choice of the sub-region did not show a clear trend (data not shown). However, the proportion of crop models where the aggregation effects followed the order of the resolution was lower in the sub-regions (*P*: 18.3%, 21.8% and 26.6% for C0:R4, C1:R3 and z50, respectively).

3.4.4. Crop model interaction with production situation

Crop models differed in their sensitivity to climate input data aggregation across production situations (Tables 5 & 6). While most models showed no clear trend, aggregation effects followed a specific order in the case of few models: increasing limitations led to more positive aggregation effects in HERMES and LandscapeDNDC for both wheat and maize and for MONICA in the case of maize, whereas APSIM and APSIM(modified) were not altered for both wheat and maize and MCWLA in the case of wheat. For the crops simulated, aggregation effects of SIMPLACE<LINTUL5>, DailyDayCent, COUP and Apsim-NW heat decreased with increasing limitation in the production situation, whereas STICS, EPIC and AquaCrop did not alter or showed an increasing range.

3.5. Model interaction with climate variable importance for projection

Using differences in climate variables and their spatial variances as independent variables for PLS regression led to model-specific sets of variables which are most determinant for single-year aggregation effects when wheat or maize yield are simulated (Tables 5 & 6). The explained variance by PLS varied between crops, models and production situations. For instance, the explained variance was 60, 91 and 82% of the single-year aggregation effects in the wheat yields simulated by LandscapeDNDC for potential, water-limited and nitrogen-water-limited production, respectively, whereas SIMPLACE<LINT-

Table 5. Climate variables related to aggregation effects with wheat grain yield. Nomenclature: P: potential; W: water-limited, N: nitrogen-water-limited; d: difference; v: spatial variance; Pr: precipitation sum, Tmin/Tmean/Tmax: minimum, mean, maximum air temperature; R: global radiation sum; GP: growing period (= sowing to maturity); SA: sowing to anthesis; AM: anthesis to maturity; L30A/L30M: period of 30 d before anthesis/maturity. Examples: dRSA: difference in the global radiation sum from sowing to anthesis, dvTminGP: difference in the spatial variance of the daily minimum temperature during the growing period. Variables are sorted from 1 to 5 in the order of their importance

Model	Production situation	Single year aggregation effect (difference in grain yield, t ha ⁻¹)		Explained variance	Variable 1	Variable 2	Variable 3	Variable 4	Variable 5
		Minimum	Maximum						
HERMES	P	-0.04	0.37	0.80	dRGP	dTminAM	dRL30A	dTmeanAM	dTmeanGP
	W	-0.14	0.57	0.73	dRGP	dvTmeanSA	dvTmeanGP	dTmeanGP	dvTmaxGP
	N	-0.13	0.58	0.74	dRGP	dvTmeanSA	dvTmeanGP	dTmeanGP	dvTmaxGP
MONICA	P	-0.33	0.47	0.75	dRGP	dvPrSA	dvTmaxSA	dvTmeanSA	dvPrGP
	W	-0.60	0.47	0.59	dvPrSA	dvPrGP	dTmaxSA	dvTmeanSA	dvTmaxSA
	N	-0.60	0.47	0.59	dvPrSA	dvPrGP	dTmaxSA	dvTmeanSA	dvTmaxSA
SIMPLACE<L5>	P	-0.06	0.37	0.80	dRSA	dRGP	dPrL30A	dvTmeanSA	dvTminGP
	W	-0.77	0.30	0.61	dvPrGP	dvPrSA	dTmeanSA	dvTmeanL30M	dvTminL30M
	N	-0.73	0.37	0.54	dvPrGP	dvPrSA	dTmeanSA	dvTminL30M	dvTmeanL30M
STICS	P	-0.60	0.62	0.59	dRSA	dRL30A	dTmaxL30A	dRGP	dTmeanL30A
	W	-0.58	0.58	0.61	dRSA	dRL30A	dTmaxL30A	dvTminGP	dvTmaxSA
	N	-0.56	0.62	0.60	dRSA	dRL30A	dTmaxL30A	dTmeanL30A	dvTmaxSA
MCWLA	P	-0.72	0.73	0.64	dRSA	dRGP	dRL30A	dPrGP	dvTmeanGP
	W	-0.72	0.73	0.64	dRSA	dRGP	dRL30A	dPrGP	dvTmeanGP
DayCent	P	-0.51	0.49	0.52	dRL30M	dvRL30M	dPrL30M	dTminGP	dTmaxL30M
	W	-0.48	0.47	0.35	dPL30M	dvPrGP	dTminL30M	dTmaxGP	dTmaxL30M
	N	-1.90	0.18	0.73	dRL30M	dRGP	dvTmaxGP	dvTmeanGP	dvRL30M
LandscapeDNDC	P	-2.36	0.17	0.60	dPL30M	dvPrGP	dRL30M	dvPrL30M	dvTmaxGP
	W	-0.88	0.18	0.91	dPL30M	dvPrGP	dRL30M	dvTmaxGP	dRGP
	N	-0.70	0.49	0.82	dvPrGP	dPrL30M	dRL30M	dvPrL30M	dvTmaxGP
COUP	P	-0.04	0.51	0.71	dRL30A	dRGP	dvTminGP	dRSA	dTmaxL30A
	W	-0.48	0.30	0.45	dRSA	dRL30A	dRL30M	dvTminGP	dvPrL30A
APSIM	P	-0.03	0.39	0.77	dRGP	dRSA	dvTmeanSA	dvTmaxSA	dTmeanSA
	W	-0.03	0.41	0.77	dRGP	dRSA	dvTmeanSA	dTmeanSA	dvTmaxSA
	N	-0.13	0.27	0.57	dRSA	dRGP	dRL30A	dvTmaxSA	dvTmeanSA
APSIM (modified)	P	-0.08	0.84	0.79	dRSA	dRGP	dTminAM	dvTmaxSA	dvTmeanGP
	W	-0.15	0.83	0.77	dRSA	dRGP	dTminAM	dvPrSA	dvPrGP
	N	-0.21	0.58	0.71	dRSA	dTminAM	dTmaxL30M	dvPrGP	dRGP
EPIC	P	-0.02	0.24	0.73	dRGP	dvTminGP	dvRL30M	dTmeanGP	dRL30M
	W	-0.37	0.57	0.50	dRGP	dvTminGP	dvTmaxGP	dTmeanGP	dvTmeanGP
	N	-0.27	0.25	0.18	dvPrGP	dvTminGP	dPrGP	dvRL30M	dTmaxGP
APSIM-NWHEAT	P	-0.10	0.32	0.74	dTminAM	dPrL30A	dRGP	dRSA	dRAM
	W	-0.50	0.32	0.61	dvPrSA	dvPrGP	dTmaxL30M	dPrL30M	dTmeanL30M

UL5> showed an opposite trend with 80, 61 and 54 %, respectively. Other models showed constantly high (HERMES, 73 to 80%) or mid (STICS, 59 to 61%) ranges of explained variance in aggregation effects of simulated wheat yields.

Key variables that statistically explained the variance for aggregation effects of single years were

identified by the VIP. Concerning wheat yield, most models showed the highest VIP for variables related to radiation, followed by variables related to temperature (e.g. HERMES) or again radiation (e.g. STICS, COUP, APSIM). Changes in the aggregation effects of wheat yields of STICS, for instance, are apparently driven mainly by radiation in the period before an-

Table 6. Climate variables related to aggregation effects with maize. Nomenclature follows Table 5

Model	Production situation	Single year aggregation effect (difference in grain yield, t ha ⁻¹)		Explained variance	Variable 1	Variable 2	Variable 3	Variable 4	Variable 5
		Minimum	Maximum						
HERMES	P	-0.15	1.42	0.85	dvPrGP	dTminGP	dvTmaxGP	dPrL30M	dTmaxGP
	W	-0.15	1.42	0.85	dvPrGP	dTminGP	dvTmaxGP	dPrL30M	dTmaxGP
	N	-0.06	1.97	0.83	dvTmaxGP	dvRL30M	dTminGP	dTminL30M	dvPrGP
MONICA	P	-0.71	0.30	0.55	dvRL30M	dvTmeanL30M	dTmaxGP	dvTminL30M	dRGP
	W	-0.63	0.83	0.49	dTmaxGP	dvRL30M	dvPrGP	dTmeanGP	dTminGP
	N	-0.63	0.83	0.49	dTmaxGP	dvRL30M	dvPrGP	dTmeanGP	dTminGP
SIMPLACE<L5>	P	-1.24	0.68	0.49	dTmaxGP	dTminGP	dvTmaxGP	dvPrGP	dPrGP
	W	-1.21	0.24	0.58	dTminGP	dvPrGP	dvTmaxGP	dvRL30M	dTmaxGP
	N	-1.20	0.42	0.46	dvPrGP	dTmaxGP	dTminGP	dPrL30M	dvRGP
STICS	P	-0.61	0.25	0.56	dvPrGP	dTminL30M	dRL30M	dTminGP	dTmeanGP
	W	-1.58	0.40	0.30	dvPrGP	dRGP	dPrL30M	dvRGP	dvRL30M
	N	-1.58	0.42	0.29	dvPrGP	dRGP	dvRGP	dPrL30M	dvRL30M
DayCent	P	-0.71	1.07	0.52	dvPrGP	dTmaxGP	dRL30M	dPrGP	dTmeanGP
	W	-0.71	1.07	0.52	dvPrGP	dTmaxGP	dRL30M	dPrGP	dTmeanGP
	N	-0.71	1.07	0.52	dvPrGP	dTmaxGP	dRL30M	dPrGP	dTmeanGP
LandscapeDNDC	P	0.00	0.57	0.80	dvPrGP	dvPrL30M	dPrL30M	dRGP	dvTmaxGP
	W	0.00	0.60	0.79	dvPrGP	dvPrL30M	dPrL30M	dvTmaxGP	dRGP
	N	-0.11	0.90	0.71	dvPrGP	dRGP	dPrL30M	dvTmaxGP	dvPrL30M
APSIM	P	-0.94	1.93	0.30	dPrL30M	dTmaxGP	dTmeanL30M	dRGP	dTmaxL30M
	W	-0.81	1.93	0.29	dPrL30M	dTmaxGP	dTmeanL30M	dRGP	dvPrL30M
	N	-0.80	1.92	0.29	dPrL30M	dTmaxGP	dTmeanL30M	dRGP	dvPrL30M
APSIM (modified)	P	-1.00	1.48	0.41	dTmaxGP	dvPrL30M	dTmeanL30M	dTmeanGP	dTminL30M
	W	-1.00	1.48	0.40	dTmaxGP	dvPrL30M	dTmeanL30M	dTmeanGP	dvPrGP
	N	-1.00	1.48	0.39	dTmaxGP	dvPrL30M	dTmeanL30M	dTmeanGP	dTminL30M
EPIC	P	-0.30	0.80	0.57	dvRL30M	dvTminGP	dvTminL30M	dvTmeanGP	dRGP
	W	-1.04	0.98	0.55	dvRGP	dPrGP	dPrL30M	dvRL30M	dvTmaxGP
	N	-1.04	0.98	0.55	dvRGP	dPrGP	dPrL30M	dvRL30M	dvTmaxGP
AquaCrop4.0	P	-0.40	0.55	0.74	dPGP	dvRL30M	dvPrL30M	dvRGP	dvTmaxGP
	W	-1.26	1.99	0.44	dvTminGP	dvRL30M	dvPrGP	dPrGP	dRL30M

thesis, followed by the temperature before anthesis. Few models indicated precipitation-related terms as most important, mainly for water-limited and nitrogen-water-limited runs (SIMPLACE<LINTUL5>, LandscapeDNDC, EPIC, MONICA). For maize, the climate variables with the highest VIP to explain aggregation effects are precipitation- and temperature-related variables, and less related to radiation. Furthermore, while changes in aggregation effects in wheat were mainly related directly to changes in climate variables, changes in aggregation effects in maize were related mainly to changes in the spatial variance of individual climate variables. No clear trend was obtained for the importance of model outputs (Tables S3 & S4) to explain the effects of climate input aggregation on either wheat or maize yields.

4. DISCUSSION

4.1. Data aggregation effects on regional climate statistics

As expected for homogeneous data, changes in the climate variables due to spatial aggregation did not alter the regional mean significantly, but decreased the spatial variance and the semivariance while narrowing extremes. The range estimated from semivariograms was above or in the range of the largest spatial resolution investigated. Thus, the requirement of spatial coherence in aggregating data was met. However, aggregation effects at resolutions coarser than 100 km were not investigated. Thus, without further analysis and depending on the research question, av-

eraging climate variables should probably be restricted to spatial resolutions up to the semivariogram range, which was 94 to 162 km in this study depending on the climate variable. Climate input data aggregation up to 100 km was also supported by Van Bussel et al. (2011b) and Angulo et al. (2013).

4.2. Effects of data aggregation on simulated yields

Simulated wheat and maize yields (mean of region and years) were biased when using aggregated climate input data. However, aggregation effects were small compared to the effect of production situations, year-to-year variability or variations across crop models. Aggregation effects in mean yields up to 0.2 t ha^{-1} as compared to 1 km grid cells are in line with findings of Folberth et al. (2012), who reported a decrease in mean yields of approximately 0.18 t ha^{-1} of maize after aggregating input data from approximately 7.5 to 45 km. Angulo et al. (2013) found biases in the median yield of up to 0.26 t ha^{-1} (LINTULSLIM) and 0.21 t ha^{-1} (WOFOST) due to the use of input data with resolutions ranging from 10 to 100 km, while biases from other models were lower ($<0.08 \text{ t ha}^{-1}$). Thus, aggregation effects on crop yields are on average low in all studies.

Aggregation hardly influenced the mean climate conditions, but decreased the variance of the climate data. Consequently, an impact on crop model outputs was expected through non-linear functions in the models. The low overall aggregation effect can, however, be explained as follows. Firstly, the present study is situated in a region with a humid, temperate climate favourable for crop growth, and all simulation runs used a typical cropland soil with high water retention capacity. Thus, changes in present climate extremes only slightly influenced the simulated mean regional yield. Secondly, aggregation effects may partially cancel out (Rastetter et al. 1992) at the grid cell level when several climate input variables are aggregated simultaneously, and at the regional level when effects of single grid cells cancel out over the region. However, aggregation effects have an effect at the grid cell level or on spatial patterns (Zhao et al. 2015b, this Special), which was also observed in our study. In conclusion, the low biases in simulating mean crop yields improve the confidence in applying crop models across scales for mean yield estimates of a given region in humid temperate conditions. However, the remaining biases still add to the simulation error, and they are likely to increase with climate data variance and absolute level, in-

creasing aridity of climate conditions, model complexity and sensitivity, whenever non-linear effects do not cancel out. This mean aggregation effect may therefore be best observed in stress situations as well as under near-optimum conditions.

Unlike the mean, yield variance and distribution narrowed in this study with aggregation. This is partially in contrast to Angulo et al. (2013), who found the range of the yield distribution to be only marginally influenced by spatial resolution of climate input variables. However, the study by Angulo et al. (2013) was based on climate data of a topographically uniform region in southwestern Finland with humid climate conditions. Thus, the discrepancies between influences of aggregation effects for the 2 regions (NRW and southwestern Finland) on yield distributions can be explained by the spatial variance of the climate.

4.3. Model sensitivity to data aggregation

4.3.1. Interaction of crop model and crop

For maize biomass, some models showed lower sensitivity to the climate input aggregation (e.g. MONICA, effect in maize biomass: $<1 \text{ t ha}^{-1}$), whereas other models showed stronger aggregation effects of up to 1.9 t ha^{-1} , (HERMES, APSIM). Although most models showed nearly equally positive and negative aggregation effects, in a few models the aggregation effect had a dominant direction over all spatial resolutions (e.g. dominant negative effect of input data aggregation in STICS, SIMPLACE<LINTUL5>). It is questionable whether these responses are the result of the model structure, or whether they result from model parameterizations. Finally, major differences were found between crops regarding the climate variables, which explain most of the variance of the single year aggregation effects (radiation for wheat, temperature for maize). The variance in the aggregation effects were explained in most models to ca. 60% and on few occasions up to $>80\%$ by PLS. While the crop model structure does not change largely between simulating wheat and maize, these changes in the model sensitivity again emphasize the role of model settings for the aggregation effects.

4.3.2. Interaction of crop model and time

Analysis of the aggregation effects at single-model and single-year levels (Figs. S2 & S4a – S4f) did not

reveal general trends, but underlined the high variability in model responses to climate input data aggregation. It can thus be concluded that the year-to-year variability of yields masks the aggregation effects on long-term simulated yields.

4.3.3. Interaction of crop model and production situation

While the minimum and maximum aggregation effects of AquaCrop4.0 showed a 3-fold increase from potential to water-limited production, no trend was found across production situations with DailyDayCent, APSIM_modified and SIMPLACE<LINTUL5>. However, some models (HERMES, LandscapeDNDC, MONICA, EPIC) showed a tendency towards larger negative aggregation effects on maize biomass when comparing potential and limited production. Interestingly, the variance in aggregation effects explained by PLS decreased with increasing limitations in the production situation, being on average 70.3, 62.8 and 60.9% for wheat and 57.9, 52.1 and 50.3% for maize under potential, water-limited and nitrogen-water-limited conditions. This indicates that increasing model complexity by adding sub-routines to account for additional processes potentially increases the fraction of aggregation effects, which can be regarded as not systematic, i.e. residual variability or noise. Angulo et al. (2013) proposed model-specific fingerprints in the form of yield PDFs after finding larger discrepancies among models than among aggregation levels.

While no characteristic fingerprints were found for soil input data aggregation (Angulo et al. 2014), the model-specific fingerprints remain to be validated for climate input data aggregation. Since the model fingerprint certainly is modulated by the model structure, it may be co-determined by further factors like model parameterization. Considering the different aggregation effects from similar models (Table S1: Apsim, Apsim_modified and Apsim-NWheat), aggregation effects seem to be partly the result of model parameterization. This does not support the hypothesis of model-specific fingerprints (Angulo et al. 2013). This result is similar to the findings by Gardner et al. (1982), who assumed—after testing hypothetical models of varying structure—that the level of complexity does not alter the aggregation effect noticeably. Consequently, climate data aggregation effects cannot directly be attributed to a given process when using regional, ensemble or other pooled outputs (e.g. mean of years). The processes causing the aggrega-

tion effects must thus be assessed at the process level, before generalizing the findings at coarser scales.

4.3.4. Model-specific drivers for aggregation effects

PLS regression was used to identify possible drivers of the aggregation effects on mean simulated yields, which were largely masked by the spatial and temporal variance. However, possible model candidates for further analysis could be identified since: (1) The explained variance by PLS shows which models exhibit systematic aggregation effects explainable by a low number of factors, (2) the selected predictors identified climate variables and model outputs as relevant key drivers. For instance, while for HERMES >70% of the variance in aggregation effects was explained by PLS, this was only ca. 50% for DailyDayCent. Similar results were obtained with generalized linear models (data not shown). Thus, models differ not only in their sensitivity, but also in their systematic component of aggregation effects. However, no clear general trend distinguishing crop models in their drivers for aggregation effects was found. While few models were identified as being influenced more by e.g. temperature or radiation, the attribution of these variables to processes in the model remains to be interpreted. For instance, HERMES showed aggregation effects well approximated by the duration of the growing period, which itself largely depends on crop-specific parameters (temperature sum, base temperature).

Although the structure of the models is known, a direct attribution of aggregation effects to the model structure (Table S1) fails due to the high variability of the effects. For instance, aggregation effects on average were larger for (1) simple light interception approaches than for detailed approaches, (2) models accounting for vernalization than models not considering vernalization, (3) yield formation based on harvest index than for yield formation based on other approaches (e.g. partitioning during reproductive stages). Hence, for a deeper understanding of aggregation effects and causal processes, the analysis needs to be combined with other multivariate methods (e.g. pattern recognition).

4.4. Assessment of aggregation effects

Following Pierce & Running (1995) and Rastetter et al. (1992), the aggregation effect should increase with increasing variance of the input data. Larger cli-

mate variability as well as different average climate conditions could lead to different aggregation effect distributions especially under growth-limiting conditions. While this depends on the data (type, spatial heterogeneity), it is unknown how the aggregation effects from climate data compare to those from other data types. Most of the spatial yield variability in Germany is caused by soil properties and soil–climate interactions. In order to focus solely on climate data aggregation effects, soil was not considered as a factor in this study. Aggregation effects from soil properties may therefore differ (Angulo et al. 2014) from the present findings. Pierce & Running (1995) compared the contributions of aggregated input data to the resulting bias in simulated net primary production, which was 32% due to spatially averaging climate data (topography 32%, vegetation and soils 34%). This remains to be verified for crop models.

5. CONCLUSIONS

Spatial aggregation of climate input data caused considerable aggregation effects for single models and in single years. Simulated regional yield estimates (average of region and years) were less affected. Differences in simulated mean regional yields across models and/or production situations or in single-year yields were larger than the aggregation error. The mean aggregation effects across models and years of up to 0.2 t ha^{-1} (<3%) contribute to the uncertainty of the estimate of regional yield and biomass. Nevertheless, it has been shown that the effects are systematic. Crop models differ in their sensitivity to aggregated data, showing different means and distributions of aggregation effects, which also depend on the production situation and the crop. Crop models differ in their systematic component of aggregation effects, regardless of the extent of the aggregation effect. Aggregation effects can be attributed to different sources, including climate, climate variability and model structure. Having studied a region in which precipitation rarely limits crop growth, global radiation and temperature were identified as the relevant climate variables which strongly influence the aggregation effects on wheat and maize yields, respectively.

Acknowledgements. This study was supported by the BMBF/BMELV project on ‘Modelling European Agriculture with Climate Change for Food Security (MACSUR)’ (grant no. 2812ERA115). The work was partly supported by the

Swedish Research Council for Environment, Agricultural Sciences and Spatial Planning and by strategic funding (‘Soil-Water-Landscape’) from the faculty of Natural Resources and Agricultural Sciences (Swedish University of Agricultural Sciences). We thank ACCAF for financial support. We thank Eric Casellas (RECORD team) for his computational assistance. We thank the Landesbetrieb Information und Technik Nordrhein-Westfalen for providing regional yield data, and the German Meteorological Service for providing weather data. We thank Professor Per-Erik Jansson (Royal Institute of Technology in Stockholm) for valuable advice linked to the application of the Coup-model. E.T. thanks the Royal Society of New Zealand and the Climate Change Impacts and Implications project for New Zealand (CCII) for financial support to collaborate with the INRES group at the University of Bonn. S.A. and D.C. acknowledge support from NOAA-RISA and IFPRI. F.T. and R.R. acknowledge support from the Academy of Finland, NORFASYS project (no. 268277) and PLUMES project (no. 277403).

LITERATURE CITED

- Angulo C, Rötter R, Trnka M, Pirttioja N, Gaiser T, Hlavinka P, Ewert F (2013) Characteristic ‘fingerprints’ of crop model responses to weather input data at different spatial resolutions. *Eur J Agron* 49:104–114
- Angulo C, Gaiser T, Rötter RP, Børgesen CD, Hlavinka P, Trnka M, Ewert F (2014) ‘Fingerprints’ of four crop models as affected by soil input data aggregation. *Eur J Agron* 61: 35–48
- Artan GA, Neale CMU, Tarboton DG (2000) Characteristic length scale of input data in distributed models: implications for modeling grid size. *J Hydrol (Amst)* 227:128–139
- Asseng S, Keating BA, Fillery IRP, Gregory PJ and others (1998) Performance of the APSIM-wheat model in Western Australia. *Field Crops Res* 57:163–179
- Asseng S, Jamieson PD, Kimball B, Pinter P, Sayre K, Bowden JW, Howden SM (2004) Simulated wheat growth affected by rising temperature, increased water deficit and elevated atmospheric CO₂. *Field Crops Res* 85: 85–102
- Bergez JE, Chabrier P, Gary C, Jeuffroy MH and others (2013) An open platform to build, evaluate and simulate integrated models of farming and agro-ecosystems. *Environ Model Softw* 39:39–49
- Bormann H, Breuer L, Graeff T, Huisman JA, Croke B (2009) Assessing the impact of land use change on hydrology by ensemble modelling (LUCHEM) IV: model sensitivity to data aggregation and spatial (re-)distribution. *Adv Water Resour* 32:171–192
- Brisson N, Mary B, Ripoche D, Jeuffroy MH and others (1998) STICS: a generic model for the simulation of crops and their water and nitrogen balances. 1. Theory and parameterization applied to wheat and corn. *Agronomie* 18: 311–346
- Brisson N, Launay M, Mary B, Beaudoin N (eds) (2008) Conceptual basis, formalisations and parameterization of the STICS crop model. Éditions Quae, Versailles
- Brown DG, Bian L, Walsh SJ (1993) Response of a distributed watershed erosion model to variations in input data aggregation levels. *Comput Geosci* 19:499–509
- Cale WG, O’Neill RV (1988) Aggregation and consistency problems in theoretical-models of exploitative resource competition. *Ecol Model* 40:97–109

- Cale WG, O'Neill RV, Gardner RH (1983) Aggregation error in non-linear ecological models. *J Theor Biol* 100: 539–550
- Chen C, Wang E, Yu Q (2010) Modeling wheat and maize productivity as affected by climate variation and irrigation supply in North China Plain. *Agron J* 102:1037–1049
- Chipanshi AC, Ripley EA, Lawford RG (1999) Large-scale simulation of wheat yields in a semi-arid environment using a crop-growth model. *Agric Syst* 59:57–66
- Cologne District Council (Bezirksregierung Köln) (2013) Nordrhein-Westfalen in Zahlen und Geodaten. Available at www.bezreg-koeln.nrw.de/brk_internet/publikationen/abteilung07/pub_geobasis_nrw.pdf (accessed on 15 December 2014)
- Conrad Y, Fohrer N (2009) Modelling of nitrogen leaching under complex winter wheat and red clover crop rotation on a drained agricultural field. *Phys Chem Earth* 34: 530–540
- De Wit AJW, Boogaard HL, Van Diepen CA (2005) Spatial resolution of precipitation and radiation: the effect on regional crop yield forecasts. *Agric For Meteorol* 135: 156–168
- Del Grosso SJ, Parton WJ, Mosier AR, Hartman MD, Brenner J, Ojima DS, Schimel DS (2001) Simulated interaction of carbon dynamics and nitrogen trace gas fluxes using the DAYCENT model. In: Schaffer M (ed) *Modeling carbon and nitrogen dynamics for soil management*. CRC Press, Boca Raton, FL, p 303–332
- Del Grosso SJ, Parton W, Mosier AR, Walsh MK, Ojima D, Thornton PE (2006) DAYCENT national scale simulations of N₂O emissions from cropped soils in the USA. *J Environ Qual* 35:1451–1460
- Ershadi A, McCabe MF, Evans JP, Walker JP (2013) Effects of spatial aggregation on the multi-scale estimation of evapotranspiration. *Remote Sens Environ* 131:51–62
- Evans LT, Fisher RA (1999) Yield potential: its definition, measurement, and significance. *Crop Sci* 39:1544–1551
- Ewert F, Van Ittersum MK, Heckelet T, Therond O, Bezlepkin I, Andersen E (2011) Scale changes and model linking methods for integrated assessment of agri-environmental systems. *Agric Ecosyst Environ* 142:6–17
- Eyshi Rezaei E, Siebert S, Ewert F (2015) Impact of data resolution on heat and drought stress simulated for winter wheat in Germany. *Eur J Agron* 65:69–82
- Folberth C, Yang H, Wang X, Abbaspour KC (2012) Impact of input data resolution and extent of harvested areas on crop yield estimates in large-scale agricultural modeling for maize in the USA. *Ecol Model* 235–236:8–18
- Gardner RH, Cale WG, O'Neill RV (1982) Robust analysis of aggregation error. *Ecology* 63:1771–1779
- Gong X, Barnston AG, Ward MN (2003) The effect of spatial aggregation on the skill of seasonal precipitation forecasts. *J Clim* 16:3059–3071
- Guo L, Dai J, Ranjekar S, Xu J, Luedeling E (2013) Response of chestnut phenology in China to climate variation and change. *Agric For Meteorol* 180:164–172
- Haas E, Klatt S, Fröhlich A, Kraft P and others (2012) LandscapeDNDC: a process model for simulation of biosphere-atmosphere-hydrosphere exchange processes at site and regional scale. *Landscape Ecol* 28:615–636
- Hansen JW, Jones JW (2000) Scaling-up crop models for climate variability applications. *Agric Syst* 65:43–72
- Hansen JW, Challinor A, Ines A, Wheeler T, Moron V (2006) Translating climate forecasts into agricultural terms: advances and challenges. *Clim Res* 33:27–41
- Haverkamp S, Fohrer N, Frede HG (2005) Assessment of the effect of land use patterns on hydrologic landscape functions: a comprehensive GIS-based tool to minimize model uncertainty resulting from spatial aggregation. *Hydrol Process* 19:715–727
- Heuvelink GBM, Pebesma EJ (1999) Spatial aggregation and soil process modelling. *Geoderma* 89:47–65
- Hoffmann H, Rath T (2012) Meteorologically consistent bias correction of climate time series for agricultural models. *Theor Appl Climatol* 110:129–141
- Hoffmann H, Rath T (2013) Future bloom and blossom frost risk for *Malus domestica* considering climate model and impact model uncertainties. *PLoS ONE* 8 doi:10.1371/journal.pone.0075033
- Holzworth DP, Huht NI, De Voil PG, Zurcher EJ and others (2014) APSIM—evolution towards a new generation of agricultural systems simulation. *Environ Model Softw* 62: 327–350
- Jansson PE, Karlberg L (2004) Coupled heat and mass transfer model for soil–plant–atmosphere systems. Royal Institute of Technology, Department of Civil and Environmental Engineering, Stockholm. Available at <http://www2.lwr.kth.se/Vara%20Datorprogram/CoupModel/NetHelp/default.htm> (accessed on 15 December 2014)
- Keating BA, Carberry PS, Hammer GL, Probert ME and others (2003) An overview of APSIM, a model designed for farming systems simulation. *Eur J Agron* 18:267–288
- Kersebaum KC (2007) Modelling nitrogen dynamics in soil-crop systems with HERMES. *Nutr Cycl Agroecosyst* 77: 39–52
- Kersebaum KC (2011) Special features of the HERMES model and additional procedures for parameterization, calibration, validation, and applications. In: Ahuja LR, Ma L (eds) *Methods of introducing system models into agricultural research*. Advances in Agricultural Systems Modeling Series 2. American Society of Agronomy, Crop Science Society of America, Soil Science Society of America, Madison, WI, p 65–94
- Kraus D, Weller S, Klatt S, Haas E, Wassmann R, Kiese R, Butterbach-Bahl K (2015) A new LandscapeDNDC biogeochemical module to predict CH₄ and N₂O emissions from lowland rice and upland cropping systems. *Plant Soil* 386:125–149
- Leopold U, Heuvelink GBM, Tiktak A, Finke PA, Schoumans O (2006) Accounting for change support in spatial accuracy assessment of modelled soil mineral phosphorus concentration. *Geoderma* 130:368–386
- Lorite IJ, Mateos L, Fereres E (2005) Impact of spatial and temporal aggregation of input parameters on the assessment of irrigation scheme performance. *J Hydrol (Amst)* 300:286–299
- Luedeling E, Gassner A (2012) Partial Least Squares Regression for analyzing walnut phenology in California. *Agric For Meteorol* 158–159:43–52
- Meentemeyer V (1989) Geographical perspectives of space, time, and scale. *Landscape Ecol* 3:163–173
- Minasny B, McBratney AB (2005) The Matérn function as general model for soil variograms. *Geoderma* 128: 192–207
- Nendel C, Berg M, Kersebaum KC, Mirschel W and others (2011) The MONICA model: testing predictability for crop growth, soil moisture and nitrogen dynamics. *Ecol Model* 222:1614–1625
- Nendel C, Wieland R, Mirschel W, Specka X, Guddat C, Kersebaum KC (2013) Simulating regional winter wheat

- yields using input data of different spatial resolution. *Field Crops Res* 145:67–77
- Nungesser MK, Joyce LA, McGuire AD (1999) Effects of spatial aggregation on predictions of forest climate change response. *Clim Res* 11:109–124
 - Parton WJ, Holland EA, Del Grosso SJ, Hartman MD and others (2001) Generalized model for NO_x and N₂O emissions from soils. *J Geophys Res* 106:17403–17420
 - Pierce LL, Running SW (1995) The effects of aggregating subgrid land-surface variation on large-scale estimates of net primary production. *Landscape Ecol* 10:239–253
 - Raes D, Steduto P, Hsiao TC, Fereres E (2009) AquaCrop - the FAO crop model to simulate yield response to water. II. Main algorithms and software description. *Agron J* 101:438–447
 - Rastetter EB, King AW, Cosby BJ, Hornberger GM, O'Neill RV, Hobbie JE (1992) Aggregating fine-scale ecological knowledge to model coarser-scale attributes of ecosystems. *Ecol Appl* 2:55–70
 - Shibu ME, Leffelaar PA, van Keulen H, Aggarwal PK (2010) LINTUL3, a simulation model for nitrogen-limited situations: application to rice. *Eur J Agron* 32:255–271
 - Statistische Ämter des Bundes und der Länder (2013) Regionaldatenbank Deutschland. Available at <https://www.regionalstatistik.de/genesis/online/logon> (accessed on 8 May 2014)
 - Steduto P, Hsiao TC, Raes D, Fereres E (2009) AquaCrop—the FAO crop model to simulate yield response to water: I. Concepts and underlying principles. *Agron J* 101:426–437
 - Syphard AD, Franklin J (2004) Spatial aggregation effects on the simulation of landscape pattern and ecological processes in southern California plant communities. *Ecol Model* 180:21–40
 - Tao F, Zhang Z (2013) Climate change, wheat productivity and water use in the North China Plain: a new superensemble-based probabilistic projection. *Agric For Meteorol* 170:146–166
 - Tao F, Yokozawa M, Zhang Z (2009) Modeling the impacts of weather and climate variability on crop productivity over a large area: a new process-based model development, optimization, and uncertainties analysis. *Agric For Meteorol* 149:831–850
 - Taylor KE (2001) Summarizing multiple aspects of model performance in a single diagram. *J Geophys Res* 106:7183–7192
 - Van Bussel LGJ, Müller C, van Keulen H, Ewert F, Leffelaar PA (2011a) The effect of temporal aggregation of weather input data on crop growth models' results. *Agric For Meteorol* 151:607–619
 - Van Bussel LGJ, Ewert F, Leffelaar PA (2011b) Effects of data aggregation on simulations of crop phenology. *Agric Ecosyst Environ* 142:75–84
 - Van Ittersum MK, Rabbinge R (1997) Concepts in production ecology for analysis and quantification of agricultural input–output combinations. *Field Crops Res* 52:197–208
 - Van Ittersum M, Leffelaar P, Van Keulen H, Kropff M, Bastiaans L, Goudriaan J (2003) On approaches and applications of the Wageningen crop models. *Eur J Agron* 18:201–234
 - Vanuytrecht E, Raes D, Steduto P, Hsiao TC and others (2014) AquaCrop: FAO'S crop water productivity and yield response model. *Environ Model Softw* 62:351–360
 - Wackernagel H (1995) *Multivariate geostatistics*. Springer-Verlag, Berlin
 - Wang E, Robertson M, Hammer G, Carberry P and others (2002) Development of a generic crop model template in the cropping system model APSIM. *Eur J Agron* 18:121–140
 - Weihermüller L, Huisman JA, Graf A, Herbst M, Vereecken H (2011) Errors in modeling carbon turnover induced by temporal temperature aggregation. *Vadose Zone J* 10:195–205
 - Williams JR (1995) The EPIC model. In: Singh VP (ed) *Computer models of watershed hydrology*. Water Resources Publications, Highland Ranch, CO, p 909–1000
 - Wold S, Sjöström M, Eriksson L (2001) PLS-regression: a basic tool of chemometrics. *Chemometr Intell Lab Syst* 58:109–130
 - Yeluripati JB, Van Oijen M, Wattenbach M, Neftel A, Ammann A, Parton WJ, Smith P (2009) Bayesian calibration as a tool for initialising the carbon pools of dynamic soil models. *Soil Biol Biochem* 41:2579–2583
 - Zhao G, Siebert S, Eyshi Rezaei E, Yan C, Ewert F (2015a) Demand for multi-scale weather data for regional crop modelling. *Agric For Meteorol* 200:156–171
 - Zhao G, Hoffmann H, Van Bussel LGJ, Enders A and others (2015b) Effect of weather data aggregation on regional crop simulation for different crops, production conditions, and response variables. *Clim Res* 65:141–157

Submitted: January 14, 2015; Accepted: July 1, 2015

Proofs received from author(s): September 7, 2015